Differences in healing patterns of the bone-implant interface between immediately and delayed placed titanium implants in mouse maxillae

Taisuke Watanabe, DDS, Graduate Student[1+], Eizo Nakagawa, DDS, PhD, Postdoctoral Fellow[1+], Kotaro Saito, DDS, PhD, Postdoctoral Fellow[1], and Hayato Ohshima, DDS, PhD, Professor[1]*

[1]Division of Anatomy and Cell Biology of the Hard Tissue, Niigata University Graduate School of Medical and Dental Sciences, Niigata, Japan

+These authors equally contributed to this work.

*corresponding author:

Hayato Ohshima, DDS, PhD

Division of Anatomy and Cell Biology of the Hard Tissue, Niigata University Graduate School of Medical and Dental Sciences, 2-5274 Gakkocho-dori, Chuo-ku, Niigata 951-8514, Japan

TEL +81-25-227-2812

FAX +81-25-227-0804

E-mail: histoman@dent.niigata-u.ac.jp

Running Head: healing pattern of immediately placed implants

Conflict of interest

The authors declare no conflict of interest.

Author Contributions: TW, Concept/Design, Data analysis/interpretation, Drafting article, Approval of article, Statistics; EN, Data analysis/interpretation, Drafting article, Approval of article, Statistics; KS, Data analysis, Drafting article, Approval of article; HO , Concept/Design, Data analysis/interpretation, Drafting article, Approval of article

ABSTRACT

Background: There are no available data on the healing process at the bone-implant interface after an immediately placed implant.

Purpose: This study was aimed to establish an animal experimental model of titanium implants placed in mouse maxillae and compare the healing pattern of the bone-implant interface after an immediately placed implant with that of a delayed placed implant.

Materials and Methods: Maxillary first molars (M1) from 4-week-old mice were extracted and replaced with the implant following drilling (immediately placed group). In contrast, M1 from 2-week-old mice were extracted, followed by the drilling and implantation after 4 weeks (delayed placed group). The decalcified samples at 0-28 days after implantation were processed for immunohistochemistry, TUNEL assay, and TRAP histochemistry. The elements and bone volume of undecalcified samples were quantitatively analyzed by an Electron Probe Micro Analyzer.

Results: Osseointegration was completed by 28 days after the procedure in both groups. There were no differences in the contact area, bone loss at the cervical area, and the rate of calcification at the bone-implant interface between the two groups.

Conclusions: This study clarified no significant differences in the chronological healing process at the bone-implant interface between the two groups at the cellular level.

KEY WORDS: dental implants, maxilla, mice (ICR), osseointegration, osteopontin, titanium, tooth extraction

INTRODUCTION

In clinical dentistry, the protocol for delayed implant placement suggests more than a 6-month healing period of the site before implant placement to allow the complete ossification of the extraction socket.[1] Immediately placed implants have been employed for more than 20 years.[2] A classification system for the timing of implant placement after tooth extraction was proposed at the Third ITI Consensus Conference in 2003,[3] and a slight modification to the classification was made later.[1] Type 1 is immediate placement. Type 2 is early placement with soft tissue healing (typically 4-8 weeks of healing). Type 3 is early placement with partial bone healing (typically 12-16 weeks of healing). Type 4 is late placement (more than 6 months of healing). Immediately placed implants have several advantages: 1) elimination of the waiting period for socket ossification, 2) fewer surgical sessions required, 3) shortened edentulous time period, 4) reduced overall cost, 5) preservation of alveolar bone height and width allowing for optimal placement in relation to implant length, width, and angulation.[2] However, several disadvantages have been reported in immediately placed implants: postoperative complications are common with immediate placement, and although there is evidence that early placement (type 2 and type 3) is associated with a lower frequency of mucosal recession compared to immediate placement (type 1),[1] the issue regarding the stability of peri-implant soft tissues is still controversial.[4, 5] Regarding the animal experimental model using dogs, the bone-implant interface following the immediately placed

implant failed to preserve the hard tissue dimension of the ridge following tooth extraction: the buccal as well as the lingual bone walls were resorbed.[6-8] Although many researchers have focused on the effects of immediate loading, surface textures, osteoplastic materials, and both bone substitute and absorbable membrane on the bone healing process following the immediately placed implant using dogs, rats, and pigs,[9-15] there is no available data on the detailed healing process of the bone-implant interface.

Even though high survival rates for implants (96.8% after 5 years) and implant-supported single crowns (SC) (94.5% after 5 years) are expected, biological and particularly technical complications are frequent.[16] Nowadays, implant-supported SC or implant-supported fixed dental prostheses (FDP) should be the first treatment option along with tooth-supported FDP.[17] The selection of an animal model serves to pre-clinically evaluate biomaterials in order to test a possible consecutive application in human patients. While small animal models such as rabbits and rats are often used, parameters like bone remodeling in large animal models such as dogs, minipigs, pigs, and goats have a much closer resemblance to human bone metabolism.[18] Osteoblasts may lay down bone on the old bone surface or on the implant surface itself around endosseous implants. The former is referred to as "distance osteogenesis," and the latter is referred to as "contact osteogenesis."[19]

Tissue response to titanium implants in the rat maxilla has been clarified at the cellular level: different patterns in bone formation were recognized at the bone-implant

interface.[20] In the lateral area with narrow gaps, bone deposition took place from the pre-existing bone towards the implant after active bone resorption by tartrate resistant acid phosphatase (TRAP)-positive osteoclasts. In contrast, new bone formation was directly deposited in the peri-implant tissue with large gaps at the bone-implant interface. These two types of bone healing are categorized as "distance osteogeneis." Interestingly, direct bone formation from the implant towards the pre-existing bone was recognizable following the recruitment of TRAP-positive osteoclast-like cells in the case of titanium implants coated with hydroxyapatite (HA) in rats: HA induces the osteoblast differentiation on the implant surface.[21] This type of bone formation is categorized as "contact osteogenesis."

Osteopontin (OPN) is a highly phosphorylated sialoprotein that is a prominent component of the mineralized extracellular matrices of bones and teeth.[22] During bone healing and osseointegration, an OPN-containing cement line has been observed at the junction between the affected surface of the older bone or implant material and the newer bone. Thus, in addition to its potential for influencing cell adhesion/dynamics in bones and teeth, OPN in cement lines may act as an interfacial adhesion promoter between apposing substrates, therein maintaining the overall integrity of bone during the bone remodeling sequence and biocompatible materials in biological composites such as teeth and osseointegrated implants.[23] However, the molecular mechanisms regulating osseointegration following implant placement remain to be clarified. To disclose the function of related

proteins including transcription factors in the process of osseointegration following implant placement from the viewpoints of the six parameters such as implant material, implant design, implant finish, status of the bone, surgical technique, and implant loading conditions,[24] the establishment of a dental implant model using mice would provide an extremely useful strategy, since transgenic mice are easily available. Furthermore, the mouse model has the advantage of reducing variation owing to individual differences. This study was aimed to establish an animal experimental model of titanium implants placed into the mouse maxilla and compare the healing pattern of the bone-implant interface after an immediately placed implant with that of a delayed placed implant.

MATERIALS AND METHODS

Animals and experimental procedure

All experiments were reviewed by the Committee on the Guidelines for Animal Experimentation of Niigata University and performed according to the recommendations or under the conditions proposed by the committee. For the immediately placed implant (immediately placed group), the upper-right first molar (M1) of 4-week-old Crlj:CD1 (ICR) mice was extracted with a pair of dental forceps with modification under anesthesia by an intraperitoneal injection of chloral hydrate (the maximum dose of 350 mg/kg) (Supplementary Figure 1a, Supplementary data 1). A cavity was prepared on the alveolar socket using a drill (a trial piece: Kentec, Tokyo, Japan) with the gripper (SPI02: Kentec) (the diameter and depth of the cavity was 1.0 mm and less than 2.0 mm, respectively: Supplementary Figure 1b, Supplementary data 1). The implant was inserted into the cavity using a screwdriver (Prosper, Kashiwazaki, Japan) after controlling the bleeding from the extraction site (Supplementary Figure 1c, d, Supplementary data 1). The untreated left M1 of the same animal was used as a control, and the extracted alveolar socket of the animal was used as the extraction group.

For the delayed implant placement (delayed placed group), the M1 of 2-week-old ICR mice was extracted in the same manner as the case of the immediately placed group and allowed to heal for 4 weeks. Subsequently, the gingiva at the position where M1 had

been removed was located by a modified needle (18G: Terumo, Tokyo, Japan), and the cavity was prepared with the implant placed in the same manner as that of the immediately placed group (Supplementary Figure 1a-i, Supplementary data 2) under anesthesia by an intraperitoneal injection of chloral hydrate (the maximum dose of 350 mg/kg).

Implant and bone characteristics and surgical technique

The establishment of osseointegration is dependent on the following parameters: 1) implant material; 2) implant design; 3) implant finish; 4) status of the bone; 5) surgical technique; 6) implant loading conditions.[24] The current implant material was titanium, and the implant design was the screw-type with a cylindrical, threaded shape (Figure 1). The current implant surface was blasted with ceramic abrasives containing mainly hydroxyapatite. The surface morphology of an implant (secondary and backscattered electron images) and the weight percent of minerals on the implant surface was analyzed using electron probe micro-analyzer (EPMA) (EPMA-8705; Shimadzu, Kyoto, Japan) (Figure 2). The weight percent of each mineral was as follows: titanium 37.7%, oxygen 31.5%, calcium 15.2%, phosphorus 8.8%, vanadium 4.1%, aluminum 2.1%, iron 0.4%, and magnesium 0.1% (Figure 2b). In the immediately placed group, the bone surrounding M1 was composed of the thin cortical bone with bone marrow in the furcation area: the mesial cortical bone faced the parotid gland, and the inferior wall of the bone was opposite the infratemporal fossa. In the control, the bone

characteristics at Week 4 were constant during the experimental periods, although the bone increased in thickness according to the elongation of roots (Figure 3a). In the delayed placed group, the cortical bone that had surrounded the mesial root disappeared (Figure 3b), although a thick cortical bone was observed in the portion near the midline (Figure 3c). The current surgical technique has been mentioned above. Regarding the last parameter, implant loading was not done.

Analyses by micro-computed tomography (μ-CT) and EPMA

μ-CT analysis (Elescan; Nittetsu Elex, Tokyo, Japan) was performed to examine the morphological changes in the surrounding bone after the removal of implants before the decalcification of samples (immediately placed group) at Week 4. The CT settings were as follows: pixel matrix 512 x 512 x 256; slice thickness 15.406 μm; projection number 900 x 32; magnification x 5.949; voltage 63 kV; electrical current 101 μA. The maxillae were reconstructed using a software program (TRI/3D Bon, Ratoc System Engineering, Tokyo, Japan) to evaluate the three-dimensionally reconstructed viewed maxillae, showing the normal configuration of bone surrounding the implant (Supplementary Figure 2). Some maxillae (immediately and delayed placed groups) at Week 4 were rinsed in 0.1 M cacodylate buffer (pH 7.4) for a couple of days and subsequently dehydrated in an ascending series of acetone and embedded in Epon 812 (Taab, Berkshire, UK). The samples were

ground down to be exposed at a position approximately equal to the central planes of the implants, and were used for chemical elements analysis using an EPMA (EPMA-8705; Shimadzu). The EPMA settings were as follows: spot size 1 μm; pixel matrix 780.20 x 780.20; voltage 15.0 kV; electrical current 0.025 μA. The mineral density of calcium, magnesium, and phosphorus in the surrounding bone between screw pitches, the bone loss (two parameters such as "a" and "b" value), and the ratio of osseointegration (contact areas between bone and implant) were analyzed: the a value was defined as the distance between the mesial enamel-cementum junction of second molars (M2) and the distal tip of osseointegration, and the b value was defined as the distance between the mesial enamel-cementum junction of M2 and the tip of the distal alveolar crest.

Histological procedure

Materials were collected in groups of 3 to 5 animals at intervals of 1, 3, 5, 7, 14 and 28 days after the operations mentioned above (n=66: Table 1). At each stage, the animals were perfused with physiological saline transcardially followed by 4% paraformaldehyde in a 0.1 M phosphate buffer (pH 7.4) under deep anesthesia by an intraperitoneal injection of chloral hydrate (350 mg/kg). The maxillae including the implants were removed *en bloc* and immersed in the same fixative for an additional 24 h. Following decalcification in a 10% EDTA-2Na solution for 2 weeks at 4°C, the specimens were dehydrated through ethanol

series and embedded in paraffin after the removal of implants, and sagittal sections of maxillae were cut at 4 μm. The paraffin sections were mounted on Matsunami adhesive silane (MAS)-coated glass (Matsunami Glass Ind., Osaka, Japan) slides and stained with hematoxylin and eosin (H&E) and processed for Azan staining.

Immunohistochemical and histochemical analyses and TUNEL assay

For the immuno-peroxidase procedure, the sections were processed for the avidin-biotin peroxidase complex (ABC) method using rabbit anti-OPN polyclonal antibody diluted to 1:5000 (LMS Co., Ltd., Tokyo, Japan). The sections were counter-stained with 0.05% methylene blue. For Ki67 immunohistochemical analysis for cell proliferation assay, the sections were processed for the ABC method using a rat anti-Ki67 monoclonal antibody diluted to 1:50 (Dako Japan, Tokyo, Japan; catalog number: K5027). The immunostained sections were counterstained with hematoxylin. For control experiments, the primary antibodies were replaced with non-immune serum or PBS. For the histochemical demonstration of TRAP activity, the azo-dye method was utilized with slight modification.[25] The paraffin sections were incubated for 15 min at room temperature in a medium comprising 0.01% naphthol AS-BI phosphatase (Na salt; Sigma Chemical, St. Louis, MO), 0.06% fast red violet LB salt (Sigma Chemical) and 50 mM l-(+)-tartaric acid in 0.2 M acetate buffer (pH 5.3). The sections were counter-stained with 0.5% methyl green. Apoptosis was

quantified by terminal deoxynucleotidyl transferase-mediated dUTP nick end labeling (TUNEL) with the ApopTag Peroxidase In Situ Apoptosis Detection Kit (Millipore; catalog number: S7100).

Statistical analysis

The numbers of Ki67-positive cells in the pulp chamber of each specimen (238×191 μm^2 grid was selected) were calculated separately. Data were obtained from 42 maxillae (17 samples from the immediately placed group and 25 samples from the delayed placed group: Table 1) for cell proliferation assay using the Ki-67 immunoreactivity. The bone loss (two parameters such as “a” and “b” value) and the ratio of osseointegration (contact areas between bone and implant) were statistically analyzed as well as the mineral density of calcium, magnesium, and phosphorus. All data were presented as the means of each group. Furthermore, the number of Ki67-positive cells among different times after the operations was compared by Bonferroni’s test (one-way analysis of variance; ANOVA) and Student’s *t*-test using statistical software (SPSS 16.0J for Windows; SPSS Japan, Tokyo, Japan).

RESULTS

On Days 1-3

In the immediately and delayed placed groups, the bone-implant interface was occupied by the inflammatory cells such as neutrophils, red blood cells, and eosinophilic matrices including a fibrin network (Figure 3d, g, h, i). An intense TRAP activity was observed on the outer and inner surface of pre-existing bone (Figure 3e) and overlapped with the immunoreaction for OPN (Figure 3f).

On Days 5-7

In the immediately placed group, the inflammatory cell infiltration gradually disappeared and spindle-shaped or flattened cells occurred in the interface between the implant surface and preexisting bone. Occasionally, the bone matrices were deposited at the bottom part of threads (Figure 4a, b, d). Numerous TRAP-positive cells appeared in the gap between the implant surface and pre-existing bone (Figure 4c, f). An immunoreaction for OPN was recognized on the surface of newly formed bone matrices (Figure 4e). In contrast, no newly formed bone matrix (Figure 4g, i) and OPN-immunoreaction were recognized on the implant surface (data not shown), although TRAP-positive cells appeared in the gap between the implant and preexisting bone in the delayed placed group (Figure 4h).

On Weeks 2-4

In the immediately and delayed placed groups, the newly formed bone matrices were observed beneath the implant surface 2 weeks after implant placement (Figure 5a, b, f, g). TRAP-positive reaction and OPN-immunoreaction were observed in the implant surface (Figure 5d, e, h). Occasionally, the bone mass appeared in the mesial side of a tooth (Figure 5c). Bone formation in the lateral area further proceeded on Week 4 (Figure 6a-i).

EPMA analyses

In the immediately and delayed placed groups, a direct contact between the implant surface and surrounding bone was completed on Week 4, although certain areas were not covered with bone to be exposed to the soft tissues including bone marrow (Figure 7a, b, g, h). The calcium, phosphorus, and magnesium levels in the surrounding bone were similar to the pre-existing bone (Figure 7c-e, i-k). The low phosphorus and titanium levels corresponded to the gap between the implant surface and surrounding bone, whereas the low calcium level was observed in the surface of the implant (Figure 7c, e, f, i, k, l). Quantitative analyses of the mineral density of calcium, magnesium, and phosphorus in the surrounding bone demonstrated no significant difference between the immediately and delayed placed groups (Figure 8). Regarding the bone loss (two parameters such as “a” and “b” value) and the ratio

of osseointegration (contact areas between bone and implant), there was no significant difference between the two groups (Figure 9).

Cell proliferative and apoptotic activities

In the immediately and delayed placed groups, the extensive TUNEL-positive reaction was observed in the surrounding tissues, and this reaction decreased in area according to the progress of healing (Figure 10a-c). Ki67 immunohistochemistry demonstrated that active cell proliferation occurred in the surrounding tissues during the early stages after the operation, although there was no significant difference between the immediately and delayed placed groups except for Day 14 (Figure 10d, e). Proliferative cells were most active at Day 3 and significantly decreased in number after Day 7 in the immediately placed group (Figure 10e).

DISCUSSION

Bone changes in the immediately placed implant group

The present study established the animal experimental model of the immediately placed implant using mice: there was no pathological bone loss in the buccal and lingual walls surrounding the implant compared with the bone surrounding the contralateral tooth, as demonstrated by μ–CT analysis. The most troublesome technical problem is to monitor and control the respiration of mice with the minimum dose of anesthetic solution so as not to strangle them by opening their mouth and holding their body. In contrast, the animal experimental model using dogs demonstrated resorption of the buccal as well as the lingual bone walls.[6-8] The discrepancy between the present and previous results is attributable to the differences in the animal species, the age of animals, and the ratio of implant size to alveolar socket volume, since several possible factors could influence differences in the outcomes between immediately and delayed placed implants (Table 2).[26-30] The age of mice used in this study was 4 weeks old when the capacity for wound healing is considerably high to affect favorably the healing process in the bone-implant interface. Furthermore, the diameter of the implant used in this study is extremely large compared with the size of roots, providing an advantage for tissue healing. Regarding the mineral density, the bone loss, and the ratio of osseointegration, there was no significant difference between the immediately and delayed placed groups. The animal experimental models would be available for the evaluation of

tissue responses to implant materials and the analyses of gene and protein expressions involved in the osseointegration. The current experimental model of the immediately placed implant using mice provide easily performed and highly reproducible experiments, since the total experimental period could be reduced compared with the experimental models using big animals or of the delayed placed implant.

Healing process in the bone-implant interface after the immediately placed implant

Osseointegration was completed by 28 days both in the immediately and delayed placed groups. However, the progress of granulation and bone formation with the appearance of TRAP-positive cells in the immediately placed group was faster than that in the delayed placed group in the initial stage (Day 5). Furthermore, the bone mass appeared occasionally in the mesial side of the tooth in the immediately placed group. These findings suggest that the periodontal tissue in the alveolar sockets partially survives to contribute to the favorable healing process in the bone-implant interface, judging from the evidence that there is a large gap between the mesial alveolar socket and implant due to the inclination toward the medial direction of the mesial root of the maxillary first molar. Thus, the viability of periodontal tissue would be a factor influencing differences in the outcomes between immediately and delayed placed implants (Table 2). Regarding cell proliferation assay, the peak reaches the maximum at Day 3 and cell proliferation significantly decreases in number after Day 5 in the immediately placed group, whereas the peak shifts to the later stages (Days 3-5) in the

delayed placed group. At Day 14, there is a significant difference in terms of cell proliferation between the two groups. These results also support the advantage regarding tissue healing in the immediately placed implant. Interestingly, the TUNEL-positive reaction corresponded to the post-operative affected areas: the extracellular matrices showed a positive reaction in addition to the TUNEL-positive apoptotic cells. This positive reaction decreased in area according to the progress of tissue healing in the bone-implant interface in both immediately and delayed placed groups. Thus, a TUNEL assay is available for the evaluation of the affected tissues following the implant surgery.

Functional significance of OPN in the bone-implant interface during osseointegration

The appearance of TRAP-positive cells precedes the osteoblast differentiation in the bone-implant interface following implantation in rats.[20, 21] The intimate relationship between the appearance of TRAP-positive osteoclast lineage cells and the osteoblast differentiation in the pulp chamber has been demonstrated in the case of tooth replantation.[25] This study confirmed the appearance of TRAP-positive cells in the bone-implant interface after Day 5 in the mouse model. Furthermore, in this study, the immunoreaction for OPN in the immediately and delayed placed groups appeared in the bone-implant surface after Day 5 and Day 7, respectively. In the case of implants coated with HA, TRAP-positive osteoclast-like cells appeared on the surface of the implant to induce direct bone formation from the implant toward the pre-existing bone. The current findings that OPN occurs on the newly formed

bone opposite to the implant suggest that OPN plays an important role in the initiation of bone formation on the implant surface. TRAP-positive osteoclast-like cells probably secrete OPN on the implant surface, since osteoclasts secrete OPN in the process of bone remodeling.

Calcium, phosphorus, and titanium levels in the bone-implant interface

It is noteworthy that the low phosphorus and titanium levels correspond to the gap between the implant surface and surrounding bone, whereas the low calcium level is recognizable in the surface of the implant. The findings indicate that the titanium dissolves out from the implant surface into the surrounding gap and subsequently it is replaced by the calcium in the implant surface. Although released titanium has been found in bone tissue in the vicinity of titanium implants,[31, 32] there are only few studies regarding the differences in the amount or types of released ions among different implant surface.[33] The current implant surface is blasted with ceramic abrasives containing mainly HA. Judging from the evidence that TRAP-positive osteoclast-lineage cells appear on the implant surface in this and other studies,[21] the recruitment of these cells by HA may be a triggering factor for the dissolution of titanium from the implant and the deposition of calcium in the implant surface. The comparison of the amount or types of released ions among different implant surfaces with/without HA remains to be clarified.

CONCLUSION

This study established the animal model of implantation in the mouse maxillae and clarified no significant differences in the chronological healing process at the bone-implant interface between immediately and delayed placed implant groups at the cellular level except for the early stages. Further animal experimental studies of implantation using transgenic mice such as OPN knock-out mice are required for the elucidation of the function of proteins or their transcriptional factors during osseointegration after implantation in the maxillae.

ACKNOWLEDGEMENTS

We are grateful to Mr. Shinichi Kenmotsu (Division of Anatomy and Cell Biology of the Hard Tissue) and Mr. Masayoshi Kobayashi (Center for Instrumental Analysis, Niigata University) for their technical assistance with sectioning and EPMA analysis, respectively.

REFERENCES

1. Chen ST, Buser D. Clinical and esthetic outcomes of implants placed in postextraction sites. *Int J Oral Maxillofac Implants* 2009; **24 Suppl**: 186-217.
2. Barzilay I. Immediate implants: their current status. *Int J Prosthodont* 1993; **6**: 169-175.
3. Hammerle CH, Chen ST, Wilson TG, Jr. Consensus statements and recommended clinical procedures regarding the placement of implants in extraction sockets. *Int J Oral Maxillofac Implants* 2004; **19 Suppl**: 26-28.
4. Tortamano P, Camargo LO, Bello-Silva MS, Kanashiro LH. Immediate implant placement and restoration in the esthetic zone: a prospective study with 18 months of follow-up. *Int J Oral Maxillofac Implants* 2010; **25**: 345-350.
5. Vignoletti F, de Sanctis M, Berglundh T, Abrahamsson I, Sanz M. Early healing of implants placed into fresh extraction sockets: an experimental study in the beagle dog. III: soft tissue findings. *J Clin Periodontol* 2009; **36**: 1059-1066.
6. Araujo MG, Lindhe J. Dimensional ridge alterations following tooth extraction. An experimental study in the dog. *J Clin Periodontol* 2005; **32**: 212-218.
7. Araujo MG, Sukekava F, Wennstrom JL, Lindhe J. Tissue modeling following implant placement in fresh extraction sockets. *Clin Oral Implants Res* 2006; **17**: 615-624.
8. Araujo MG, Wennstrom JL, Lindhe J. Modeling of the buccal and lingual bone walls of fresh extraction sites following implant installation. *Clin Oral Implants Res* 2006; **17**: 606-614.
9. Blanco J, Mareque S, Linares A, Perez J, Munoz F, Ramos I. Impact of immediate loading on early bone healing at two-piece implants placed in fresh extraction sockets: an experimental study in the beagle dog. *J Clin Periodontol* 2013; **40**: 421-429.
10. Colombo JS, Satoshi S, Okazaki J, Crean SJ, Sloan AJ, Waddington RJ. In vivo monitoring of the bone healing process around different titanium alloy implant surfaces placed into fresh extraction sockets. *J Dent* 2012; **40**: 338-346.
11. Blanco J, Linares A, Perez J, Munoz F. Ridge alterations following flapless immediate implant placement with or without immediate loading. Part II: a histometric study in the Beagle dog. *J Clin Periodontol* 2011; **38**: 762-770.
12. Kotenko MV, Meysner LL. Morphological features of peri-implant tissue after placement of dental implants into the extraction socket. *Bull Exp Biol Med* 2011; **151**: 492-497.
13. Barone A, Ricci M, Calvo-Guirado JL, Covani U. Bone remodelling after regenerative procedures around implants placed in fresh extraction sockets: an experimental study in Beagle dogs. *Clin Oral Implants Res* 2011; **22**: 1131-1137.
14. Vignoletti F, de Sanctis M, Berglundh T, Abrahamsson I, Sanz M. Early healing of implants placed into fresh extraction sockets: an experimental study in the beagle dog. II:

ridge alterations. *J Clin Periodontol* 2009; **36**: 688-697.
15. Vignoletti F, Johansson C, Albrektsson T, De Sanctis M, San Roman F, Sanz M. Early healing of implants placed into fresh extraction sockets: an experimental study in the beagle dog. De novo bone formation. *J Clin Periodontol* 2009; **36**: 265-277.
16. Jung RE, Pjetursson BE, Glauser R, Zembic A, Zwahlen M, Lang NP. A systematic review of the 5-year survival and complication rates of implant-supported single crowns. *Clin Oral Implants Res* 2008; **19**: 119-130.
17. Pjetursson BE, Bragger U, Lang NP, Zwahlen M. Comparison of survival and complication rates of tooth-supported fixed dental prostheses (FDPs) and implant-supported FDPs and single crowns (SCs). *Clin Oral Implants Res* 2007; **18 Suppl 3**: 97-113.
18. Stadlinger B, Pourmand P, Locher MC, Schulz MC. Systematic review of animal models for the study of implant integration, assessing the influence of material, surface and design. *J Clin Periodontol* 2012; **39 Suppl 12**: 28-36.
19. Davies JE. Understanding peri-implant endosseous healing. *J Dent Educ* 2003; **67**: 932-949.
20. Futami T, Fujii N, Ohnishi H, Taguchi N, Kusakari H, Ohshima H, Maeda T. Tissue response to titanium implants in the rat maxilla: ultrastructural and histochemical observations of the bone-titanium interface. *J Periodontol* 2000; **71**: 287-298.
21. Shirakura M, Fujii N, Ohnishi H, Taguchi Y, Ohshima H, Nomura S, Maeda T. Tissue response to titanium implantation in the rat maxilla, with special reference to the effects of surface conditions on bone formation. *Clin Oral Implants Res* 2003; **14**: 687-696.
22. Sodek J, Ganss B, McKee MD. Osteopontin. *Crit Rev Oral Biol Med* 2000; **11**: 279-303.
23. McKee MD, Nanci A. Osteopontin at mineralized tissue interfaces in bone, teeth, and osseointegrated implants: ultrastructural distribution and implications for mineralized tissue formation, turnover, and repair. *Microsc Res Tech* 1996; **33**: 141-164.
24. Albrektsson T, Branemark PI, Hansson HA, Lindstrom J. Osseointegrated titanium implants. Requirements for ensuring a long-lasting, direct bone-to-implant anchorage in man. *Acta Orthop Scand* 1981; **52**: 155-170.
25. Tsukamoto-Tanaka H, Ikegame M, Takagi R, Harada H, Ohshima H. Histochemical and immunocytochemical study of hard tissue formation in dental pulp during the healing process in rat molars after tooth replantation. *Cell Tissue Res* 2006; **325**: 219-229.
26. Ferrus J, Cecchinato D, Pjetursson EB, Lang NP, Sanz M, Lindhe J. Factors influencing ridge alterations following immediate implant placement into extraction sockets. *Clin Oral Implants Res* 2010; **21**: 22-29.
27. Schropp L, Kostopoulos L, Wenzel A. Bone healing following immediate versus delayed placement of titanium implants into extraction sockets: a prospective clinical study. *Int J Oral Maxillofac Implants* 2003; **18**: 189-199.

28. Botticelli D, Berglundh T, Lindhe J. Hard-tissue alterations following immediate implant placement in extraction sites. *J Clin Periodontol* 2004; **31**: 820-828.
29. Polizzi G, Grunder U, Goene R, Hatano N, Henry P, Jackson WJ, Kawamura K, Renouard F, Rosenberg R, Triplett G, Werbitt M, Lithner B. Immediate and delayed implant placement into extraction sockets: a 5-year report. *Clin Implant Dent Relat Res* 2000; **2**: 93-99.
30. Chen ST, Darby IB, Adams GG, Reynolds EC. A prospective clinical study of bone augmentation techniques at immediate implants. *Clin Oral Implants Res* 2005; **16**: 176-184.
31. Lodding AR, Fischer PM, Odelius H. Secondary ion mass spectrometry in the study of biomineralizations and biomaterials. *Analytica Chimica Acta* 1990; **241**: 299-314.
32. Osborn JF, Willich P, Meenen N. The release of titanium into human bone from a titanium implant coated with plasma-sprayed titanium. Elsevier Science Publishers B.V. Amsterdam
33. Wennerberg A, Ide-Ektessabi A, Hatkamata S, Sawase T, Johansson C, Albrektsson T, Martinelli A, Sodervall U, Odelius H. Titanium release from implants prepared with different surface roughness. *Clin Oral Implants Res* 2004; **15**: 505-512.

FIGURE LEGENDS

Figure 1 The implant design is the screw-type with cylindrical, threaded shape; the implant surface is blasted with ceramic abrasives containing mainly hydroxyapatite.

Figure 2 The surface morphology of an implant (**a, c, d**) and the weight percent of minerals on the implant surface (**b**) demonstrated by EPMA. (**a**) A backscattered electron image of the implant. (**b**) Quantitative data of minerals on the implant surface. (**c, d**) A secondary electron image of the implant. (**d**) Figures **d** is higher magnification of the *boxed areas* in **c**. *Bars* 200 μm (**a**), 50 μm (**c**), 10 μm (**d**)

Figure 3 Hematoxylin and eosin (H&E)- (**a-c, h**) and Azan-staining (**d, g, i**), tartrate-resistant acid phosphatase (TRAP) reaction (**e**), and osteopontin (OPN)-immunoreactivity (**f**) in a control tooth with surrounding tissues (**a**), the alveolar bone after tooth extraction (**b, c**), and the tissues surrounding immediately (**d-f**) and delayed placed implants (**g-i**) at 1 day (**d-i**), 2 (**b**), and 4 (**a, c**) weeks after implantation (*AB* alveolar bone, *IS* implant space, *M2* maxillary second molar, *NC* nasal cavity, *PG* parotid grand). The rectangles in figures **b** and **c** indicate the position of implants. (**a)** The bone surrounding a maxillary first molar (*M1*) is composed of the thin cortical bone with bone marrow in the furcation area. (**b**) The cortical bone that has surrounded the mesial root disappears. (**c**) The thick cortical bone is observed in the portion near the midline. (**d, g, h, i**) The bone-implant interface is occupied by the inflammatory cells such as neutrophils, red blood cells, and

eosinophilic matrices including a fibrin network. Figure **h** is a higher magnification of the *boxed area* in figure **g**. (**e, f**) An intense TRAP activity is observed on the outer and inner surface of pre-existing bone and overlapped with the immunoreaction for OPN. *Bars* 500 μm (**a-d, g**), 100 μm (**e, f**), 50 μm (**h, i**)

Figure 4 H&E- (**i**) and Azan-staining (**a, b, d, g**), TRAP reaction (**c, f, h**), and OPN-immunoreactivity (**e**) in the tissues surrounding immediately (**a-f**) and delayed placed implants (**g-i**) at 5 days after implantation (*B* bone, *IS* implant space, *PG* parotid grand). (**a, b, d)** An inflammatory cell infiltration almost disappears and spindle-shaped or flattened cells occur in the bone-implant interface; the bone matrices are deposited at the bottom part of threads (*arrows*). (**c, f**) Numerous TRAP-positive cells appear in the gap between the implant surface and pre-existing bone. (**e**) An immunoreaction for OPN is observed on the surface of newly formed bone matrices (*arrowheads*). (**g, i**) There is no bone formation on the surface of the implant. (**h**) TRAP-positive cells occur in the bone-implant interface. Figure **f** is a higher magnification of the *boxed area* in **c**. *Bars* 250 μm (**a, g**), 100 μm (**b-d**), 50 μm (**h, i**), 25 μm (**e, f**)

Figure 5 Azan-staining (**a-c, f, g**), TRAP reaction (**e**), and OPN-immunoreactivity (**d, h**) in the tissues surrounding immediately (**a-e**) and delayed placed implants (**f-h**) at 2 weeks after implantation (*B* bone, *IS* implant space, *NC* nasal cavity, *PG* parotid grand). (**a, b, f, g)** The newly formed bone matrices are observed beneath the implant surface. Figures **b,**

c, and **g** are higher magnifications of the *boxed areas* in **a, a,** and **f**, respectively. (**c**) Note the bone mass appearing in the mesial side of an implant. (**d, e, h**) TRAP-positive reaction and OPN-immunoreaction are observed on the implant surface. *Bars* 500 μm (**a, f**), 100 μm (**c**), 50 μm (**b, e, g, h**), 25 μm (**d**)

Figure 6 H&E (**e**) and Azan-staining (**a, b, g, h**), TRAP reaction (**d, f**), and OPN-immunoreactivity (**c, i**) in the tissues surrounding immediately (**a-e**) and delayed placed implants (**f-i**) at 4 weeks after implantation (*B* bone, *IS* implant space, *NC* nasal cavity). (**a-i)** Bone formation in the lateral area has proceeded. Figures **b** and **h** are higher magnifications of the *boxed areas* in **a** and **g**, respectively. *Bars* 250 μm (**a, g**), 50 μm (**b-f, h, i**)

Figure 7 Sagittal views of the tissues surrounding immediately (**a-f**) and delayed placed implants (**g-l**) at 4 weeks after implantation obtained by EPMA procedures (*M2* maxillary second molar). Figures **b** and **h** are higher magnifications of the *boxed areas* in figures **a** and **g**, respectively. (**a, b, g, h**) A direct contact between the implant surface and surrounding bone is completed, although certain areas were not covered with bone to be exposed to the soft tissues including bone marrow. (**c-e, i-k**) The calcium (**c, i**), phosphorus (**e, k**), magnesium levels (**d, j**) in the surrounding bone are similar to the pre-existing bone. (**c, e, f, i, k, l**) The low phosphorus (**e, k**) and titanium levels (**f, l**)

correspond to the gap between the implant surface and surrounding bone, whereas the low calcium level is observed in the surface of the implant (**c, i**).

Figure 8 Quantitative analyses of the mineral density of calcium, magnesium, and phosphorus in the surrounding bone showing no significant difference between the immediately and delayed placed groups. The boxes in figures **a** and **b** indicate the areas analyzed for the mineral density.

Figure 9 The bone loss (two parameters such as "a" and "b" value) and the ratio of osseointegration (contact areas between bone and implant): there is no significant difference between the two groups.

Figure 10 TUNEL- (**a-c**) and Ki67-immunoreactivities (**d**) in the tissues surrounding immediately placed implants (**a-d**) at 1 (**a**), 3 (**d**), 5 (**b**), and 14 days (**c**) after implantation and quantitative analysis of cell proliferation in the peri-implant space at 1, 3, 5, 7, and 14 days after operation (*IS* implant space). (**a-c**) The extensive TUNEL-positive reaction is observed in the surrounding tissues, and this reaction decreases in area according to the progress of healing. (**d**) Active cell proliferation occurs in the surrounding tissues during the early stages after the operation. (**e**) There is a significant difference between Day 3 and Day 7 or Day 14 in the immediate placed group ($P<0.05$). There is no significant difference between the immediately and delayed placed groups except for Day 14. *Bars* 500 μm (**a-c**), 100 μm (**d**)

Supplementary Figure 1 Sequential steps of the procedures for immediately (**a-d**) and delayed placed implants (**e-i**). (**a**) Tooth extraction. (**b, g**) Cavity preparation on the alveolar socket using a drill with the gripper. (**c, h**) Implant insertion into the cavity using a screwdriver. (**d, i**) Completion of implant placement. (**e**) Positioning of the gingiva to be removed by a modified needle. (**f**) Completion of gingival removal before cavity preparation.

Supplementary Figure 2 μCT (**a-d**) and stereoscopic images (**e-g**) of the undecalcified (**a-d**) and decalcified maxillae (**e-g**) where the implant had been placed immediately after tooth extraction (**e**) and subsequently was extracted (**a-d, f, g**) on Weeks 4 (*M1* maxillary first molar, *M2* maxillary second molar, *M3* maxillary third molar, * implant or implant space). (**a-c, e-g**) The three-dimensionally-reconstructed or stereoscopic maxillae show the normal configuration of bone surrounding the implant. (**d**) The sagittally-viewed maxilla represents the newly formed bone.

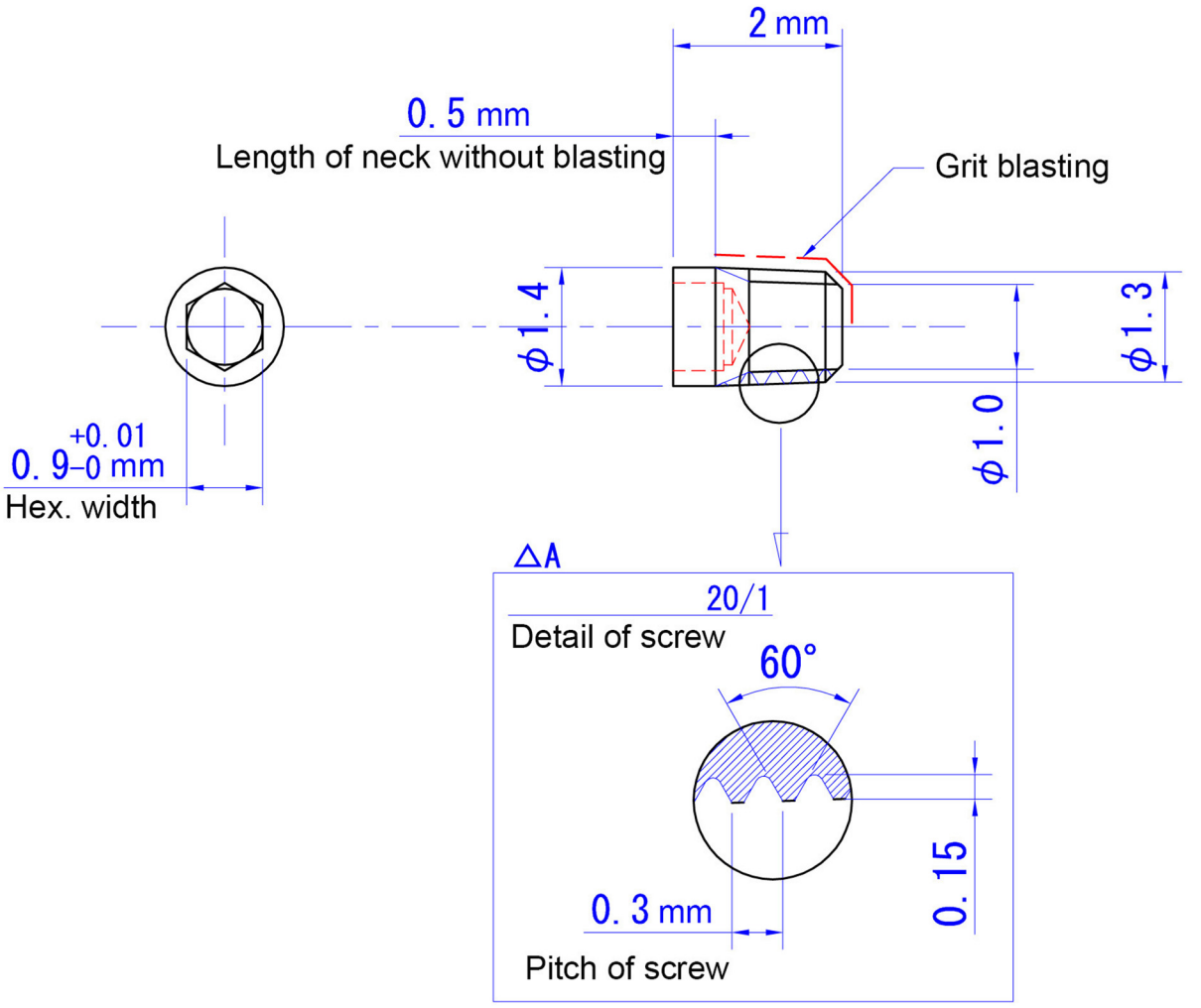
2 mm
0. 5 mm
Length of neck without blasting
Grit blasting
φ1. 4
φ1. 3
φ1. 0
+0. 01
0. 9−0 mm
Hex. width
△A
20/1
Detail of screw
60°
0. 15
0. 3 mm
Pitch of screw

Figure 1

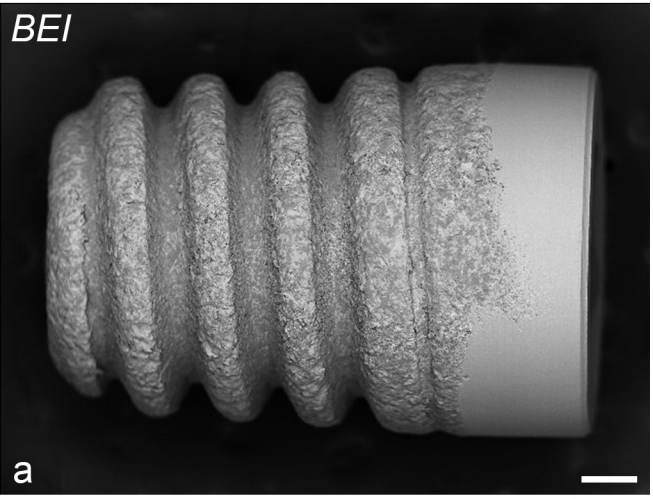
BEI
a

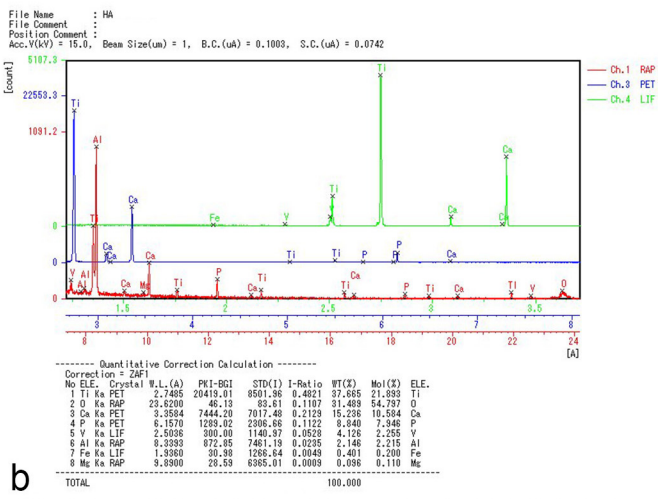
File Name : HA
File Comment :
Position Comment :
Acc.V(kV) = 15.0, Beam Size(um) = 1, B.C.(uA) = 0.1003, S.C.(uA) = 0.0742
[count]
5107.8
22553.3
1031.2
Ch.1 RAP
Ch.3 PET
Ch.4 LIF
[A]
Quantitative Correction Calculation
Correction = ZAF1
No ELE. Crystal W.L.(A) PKI-BGI STD(I) I-Ratio WT(%) Mol(%) ELE.
1 Ti Ka PET 2.7485 20419.01 8501.96 0.4821 37.665 21.893 Ti
2 O Ka RAP 23.6200 46.13 83.61 0.1107 31.489 54.797 O
3 Ca Ka PET 3.3584 7444.20 7017.48 0.2129 15.236 10.584 Ca
4 P Ka PET 6.1570 1289.02 2306.66 0.1122 8.640 7.946 P
5 V Ka LIF 2.5036 300.00 1140.97 0.0528 4.126 2.255 V
6 Al Ka RAP 8.3393 872.85 7481.19 0.0235 2.146 2.215 Al
7 Fe Ka LIF 1.9360 30.98 1266.64 0.0049 0.401 0.200 Fe
8 Mg Ka RAP 9.8900 28.59 6365.01 0.0009 0.096 0.110 Mg
TOTAL 100.000
b

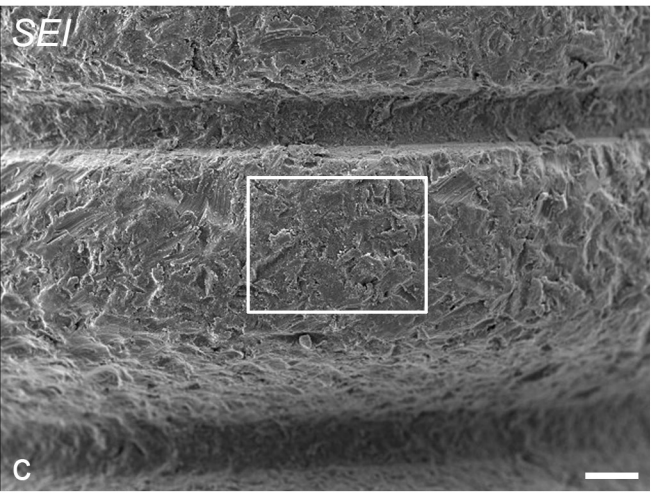
SEI
c

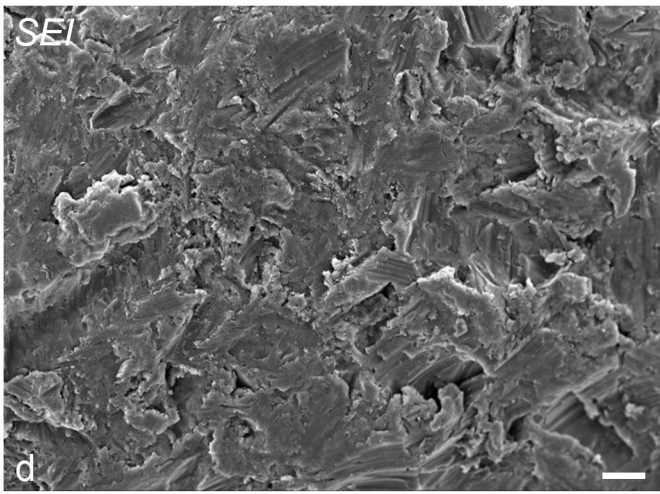
SEI
d

Figure 2

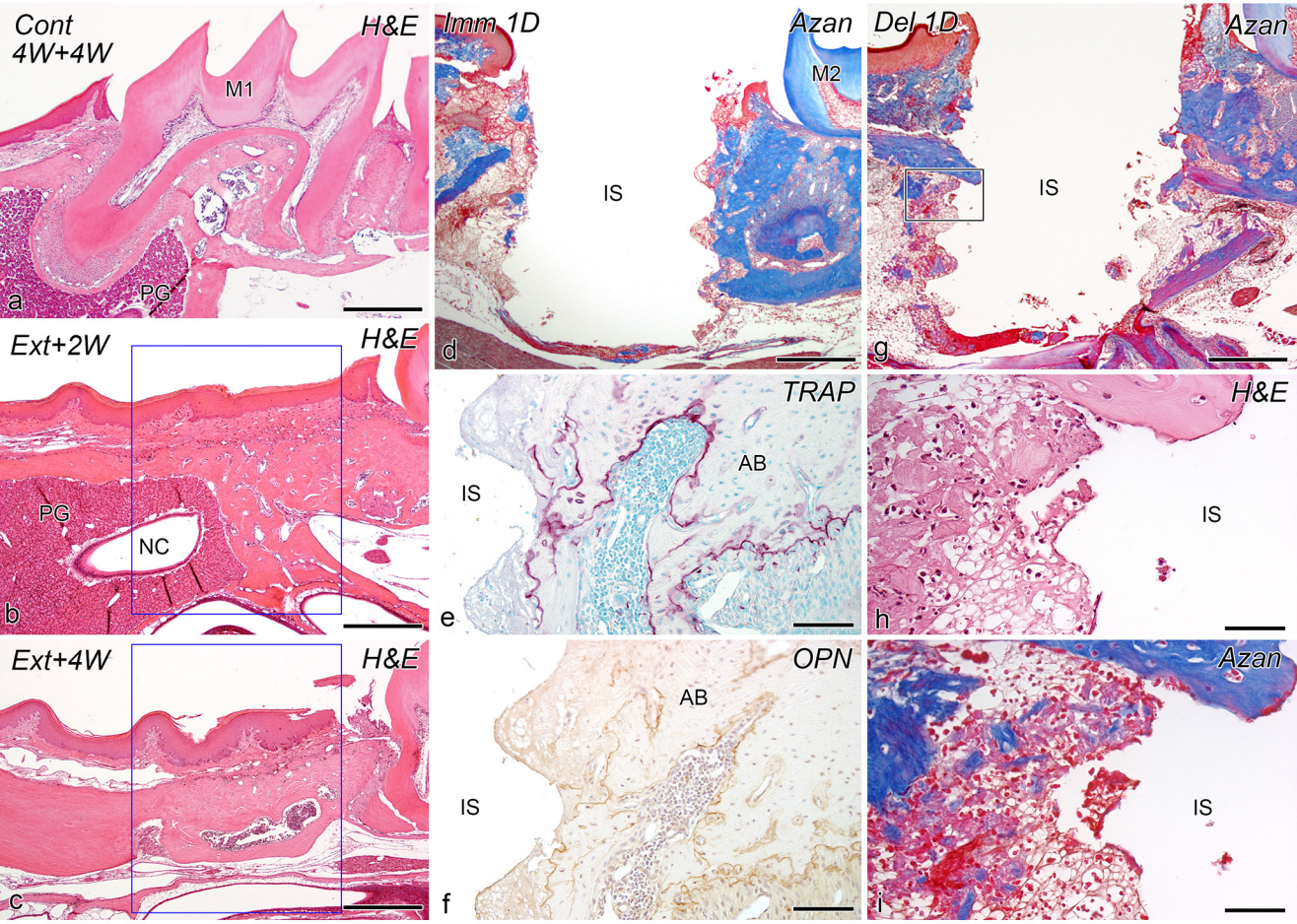
Cont
4W+4W
H&E
M1
PG
a
Imm 1D
Azan
M2
IS
d
Del 1D
Azan
IS
g
Ext+2W
H&E
PG
NC
b
TRAP
AB
IS
e
H&E
IS
h
Ext+4W
H&E
c
OPN
AB
IS
f
Azan
IS
i

Figure 3

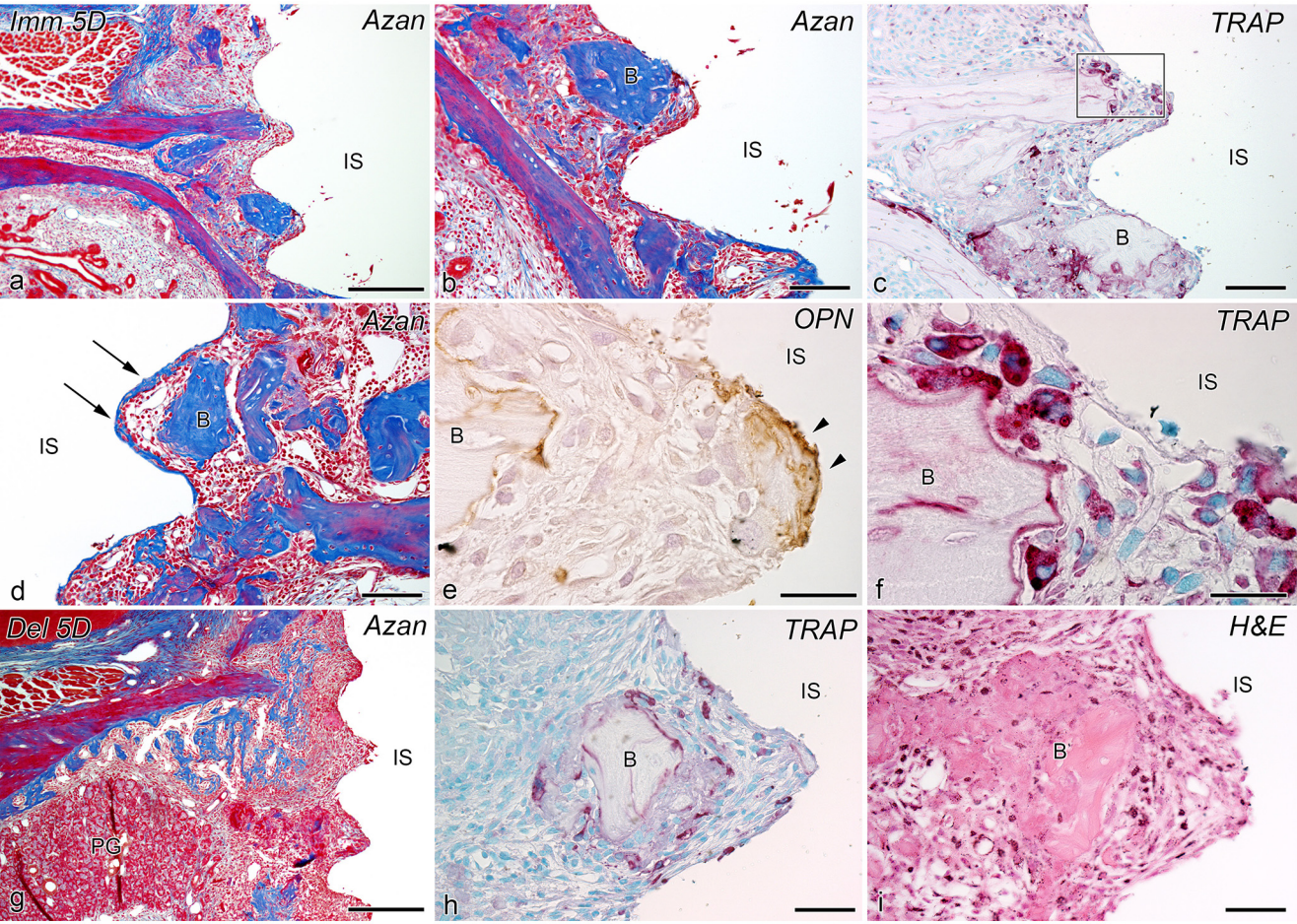
Imm 5D
Azan
IS
a
Azan
B
IS
b
TRAP
IS
B
c
Azan
B
IS
d
OPN
IS
B
e
TRAP
IS
B
f
Del 5D
Azan
IS
PG
g
TRAP
IS
B
h
H&E
IS
B
i

Figure 4

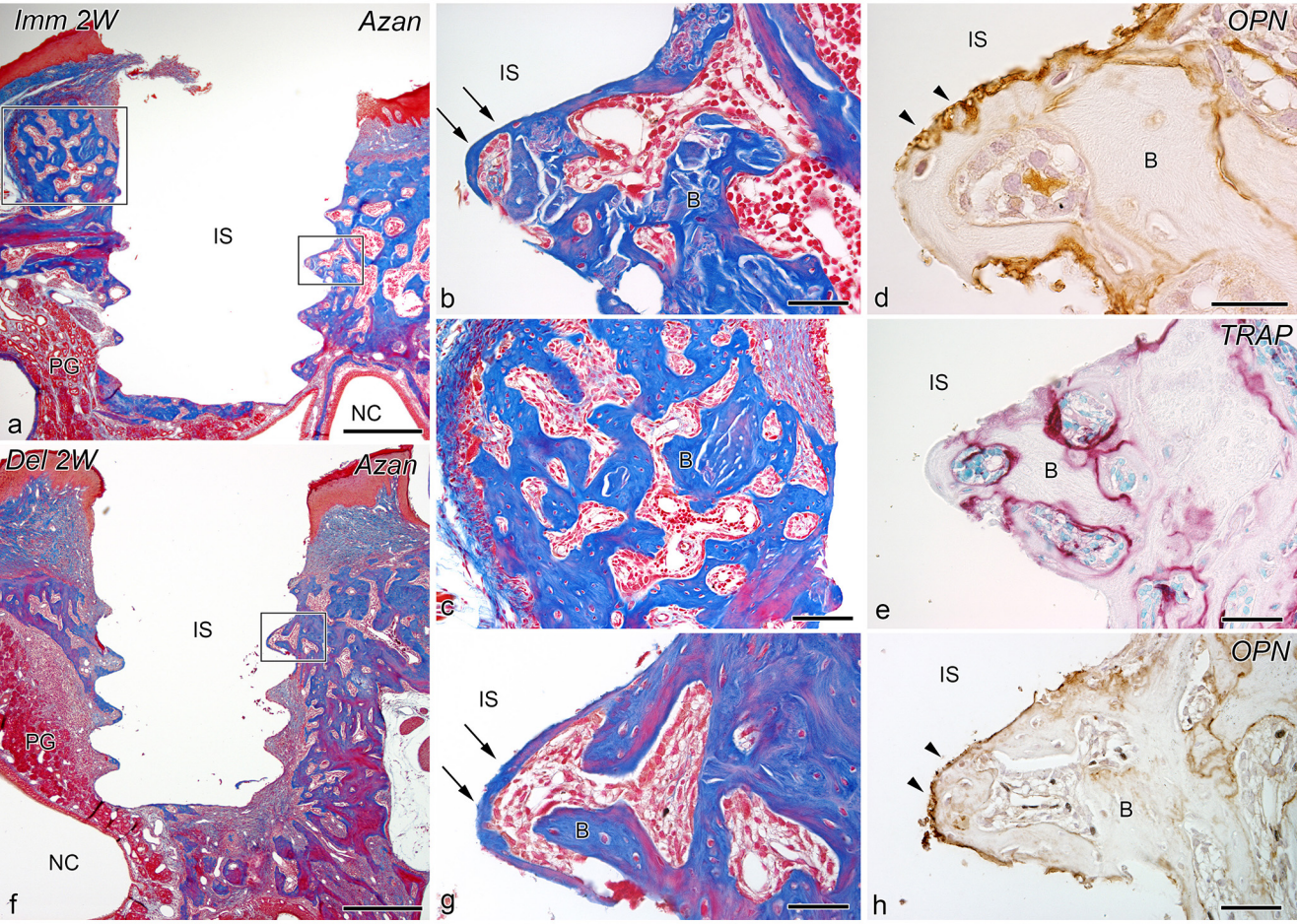
Imm 2W
Azan
IS
PG
NC
a
b
IS
B
OPN
IS
B
d
B
c
TRAP
IS
B
e
Del 2W
Azan
IS
PG
NC
f
IS
B
g
OPN
IS
B
h

Figure 5

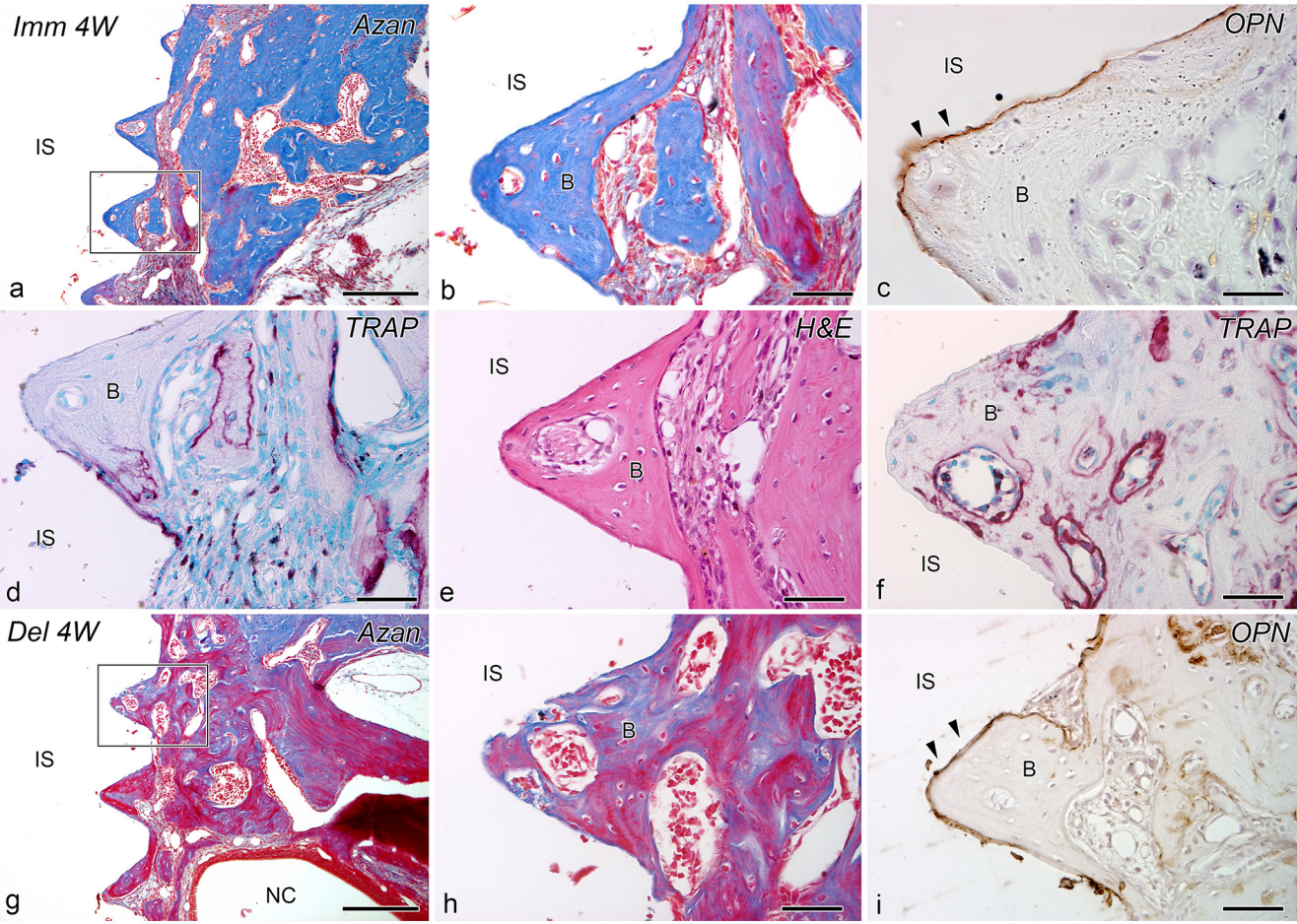
Imm 4W
Azan
IS
a
IS
B
b
OPN
IS
B
c
TRAP
B
IS
d
H&E
IS
B
e
TRAP
B
IS
f
Del 4W
Azan
IS
NC
g
IS
B
h
OPN
IS
B
i

Figure 6

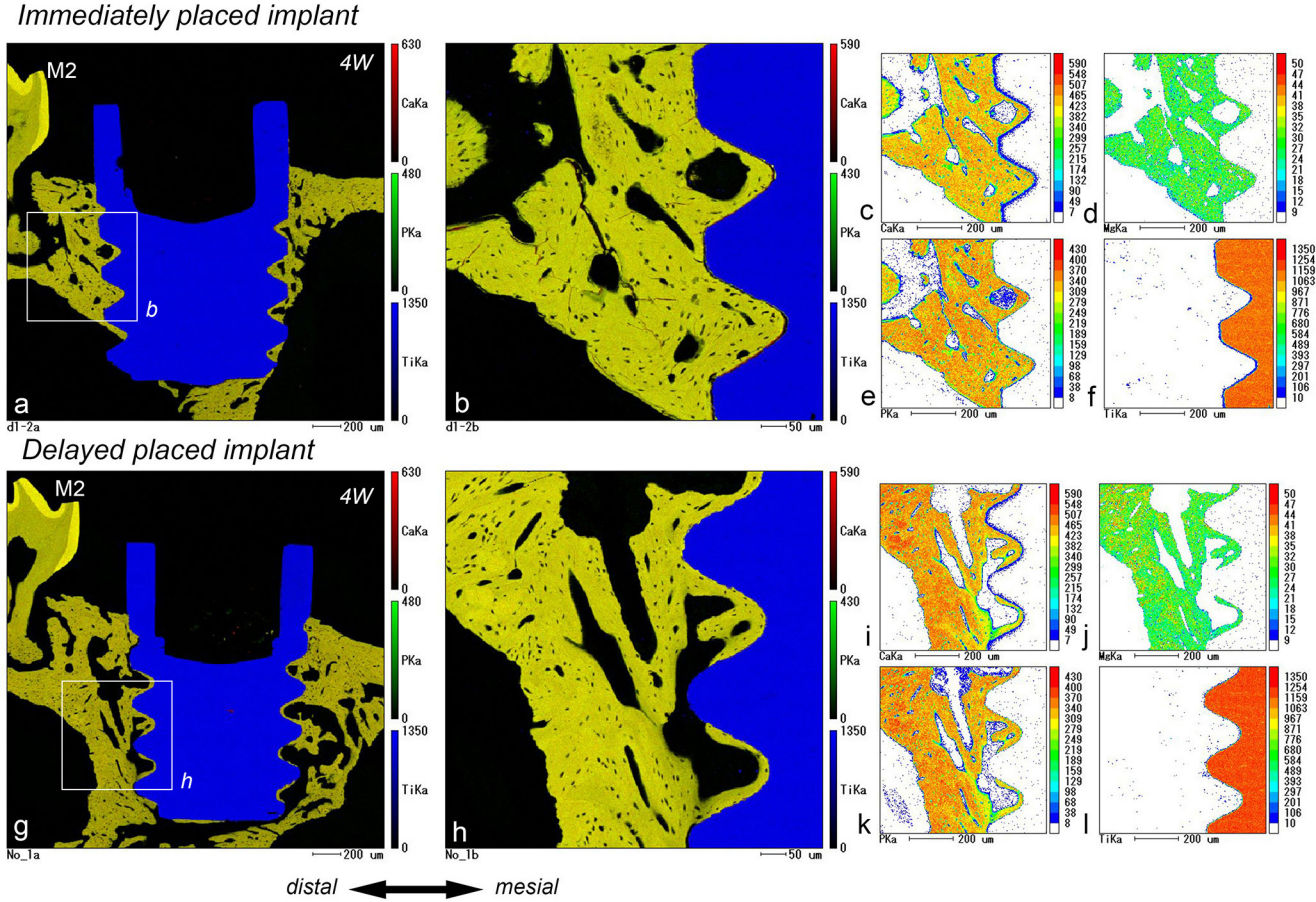
Immediately placed implant
M2
4W
b
a
d1-2a
200 um
CaKa
PKa
TiKa
630
480
1350
0
b
d1-2b
50 um
590
430
c
d
e
f
CaKa
PKa
MgKa
TiKa
200 um
Delayed placed implant
M2
4W
h
g
No_1a
200 um
h
No_1b
50 um
i
j
k
l
distal
mesial

Figure 7

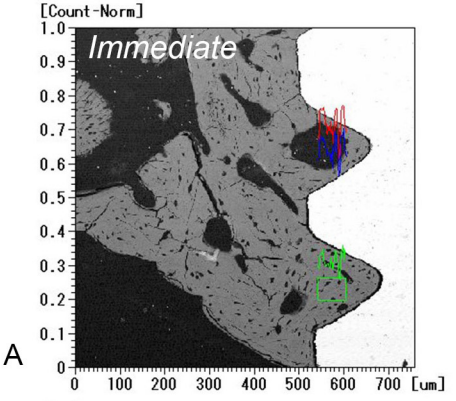
[Count-Norm]
Immediate
0 100 200 300 400 500 600 700 [um]

A

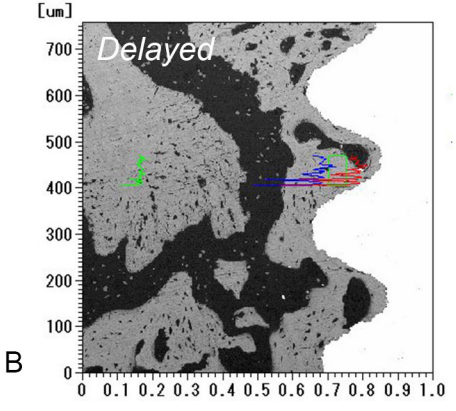
[um]
Delayed
0 0.1 0.2 0.3 0.4 0.5 0.6 0.7 0.8 0.9 1.0

B

C

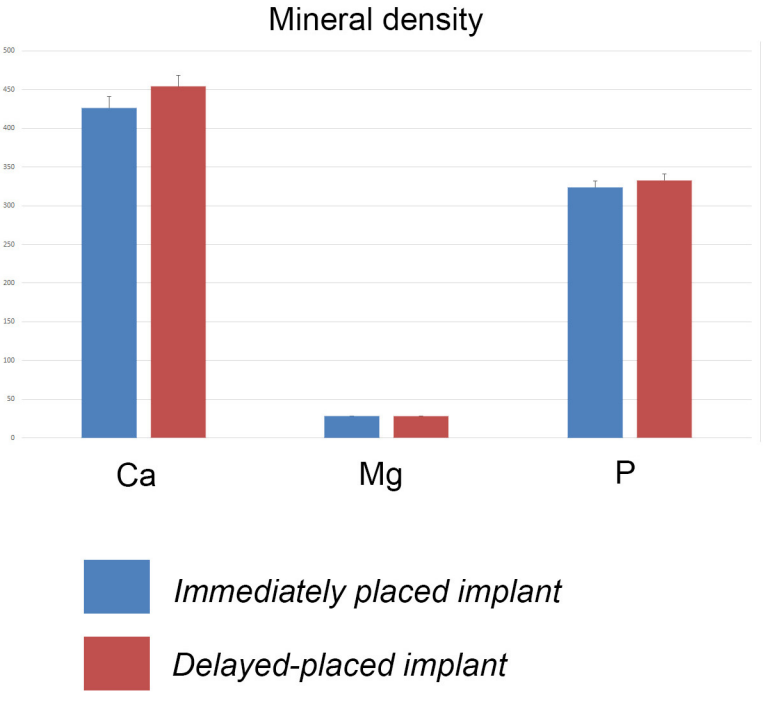
Mineral density
Ca
Mg
P
Immediately placed implant
Delayed-placed implant

Figure 8

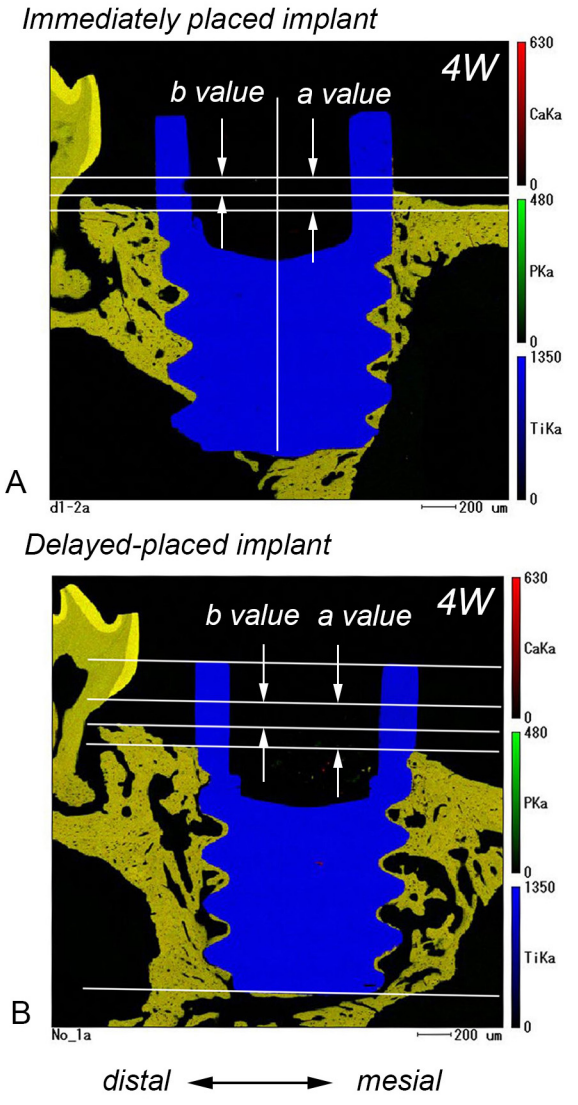
Immediately placed implant
4W
b value
a value
630
CaKa
0
480
PKa
0
1350
TiKa
0
d1-2a
200 um
A
Delayed-placed implant
4W
b value
a value
630
CaKa
0
480
PKa
0
1350
TiKa
0
No_1a
200 um
B
distal
mesial

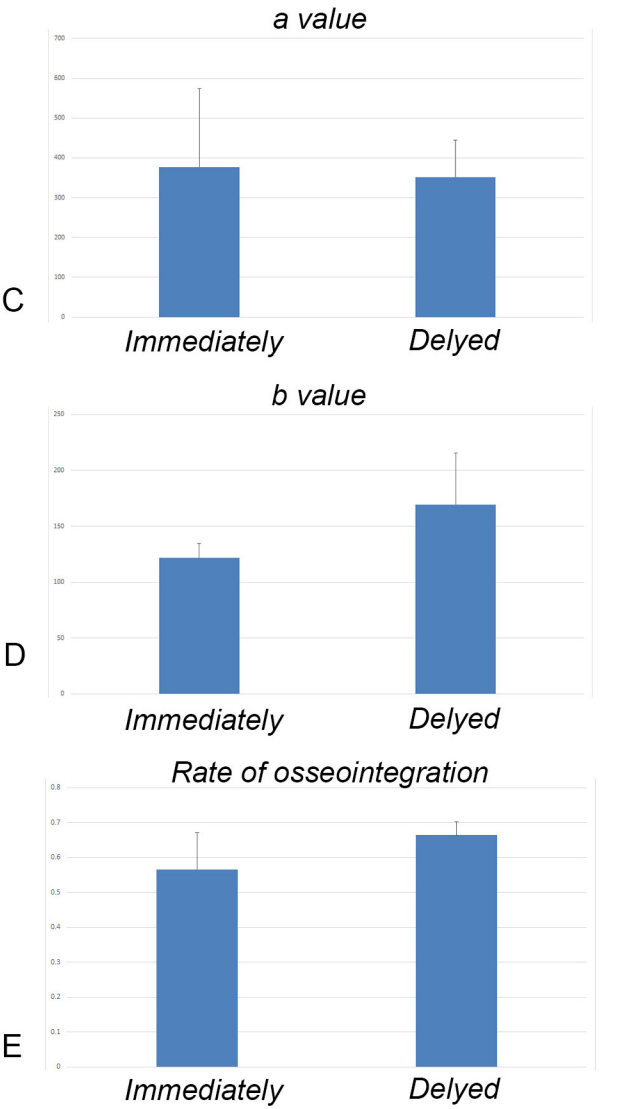
a value
C
Immediately
Delyed
b value
D
Immediately
Delyed
Rate of osseointegration
E
Immediately
Delyed

Figure 9

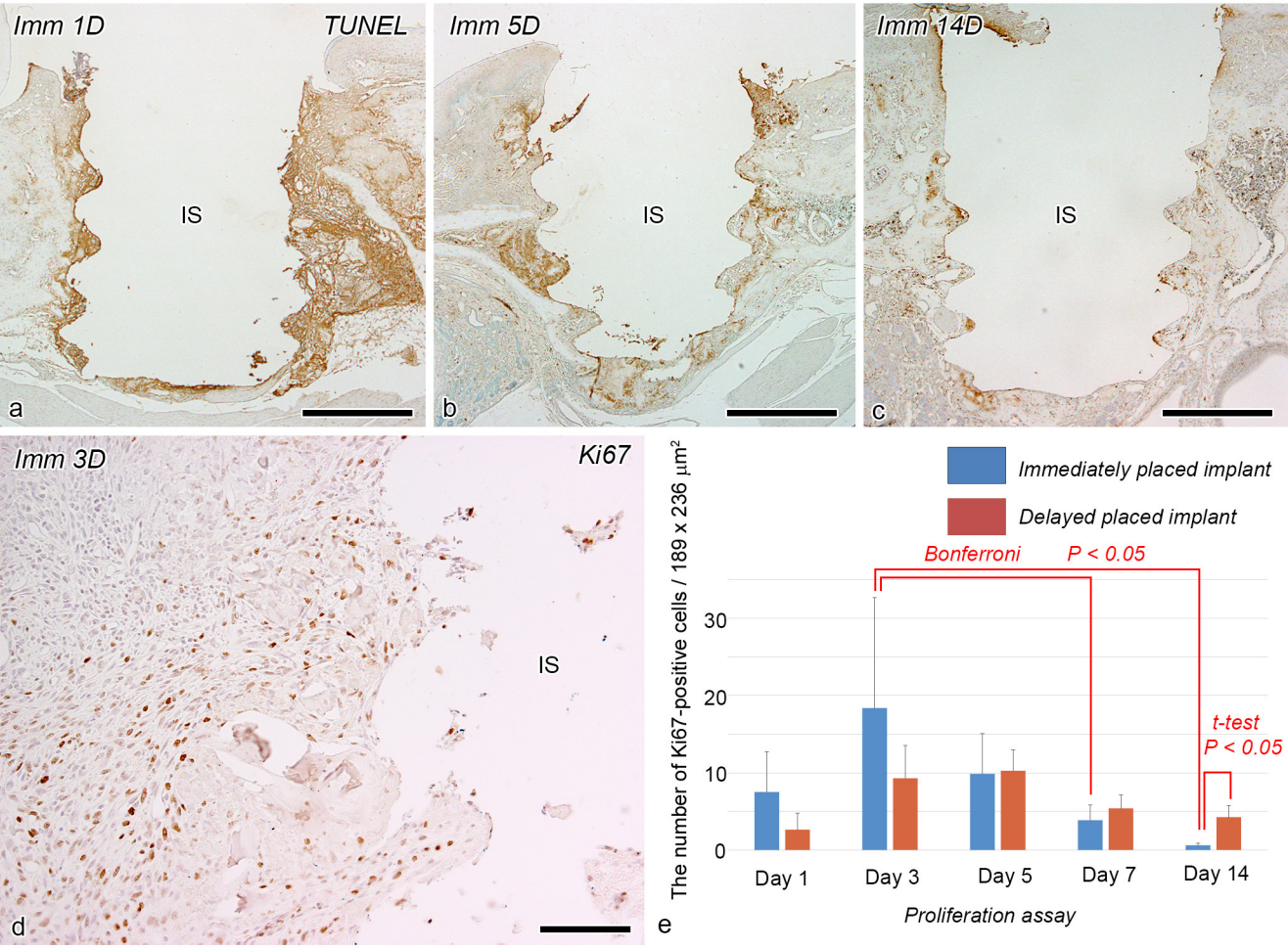
Imm 1D
TUNEL
IS
a
Imm 5D
IS
b
Imm 14D
IS
c
Imm 3D
Ki67
IS
d
Immediately placed implant
Delayed placed implant
Bonferroni
P < 0.05
t-test
P < 0.05
The number of Ki67-positive cells / 189 x 236 µm²
30
20
10
0
Day 1
Day 3
Day 5
Day 7
Day 14
Proliferation assay
e

Figure 10

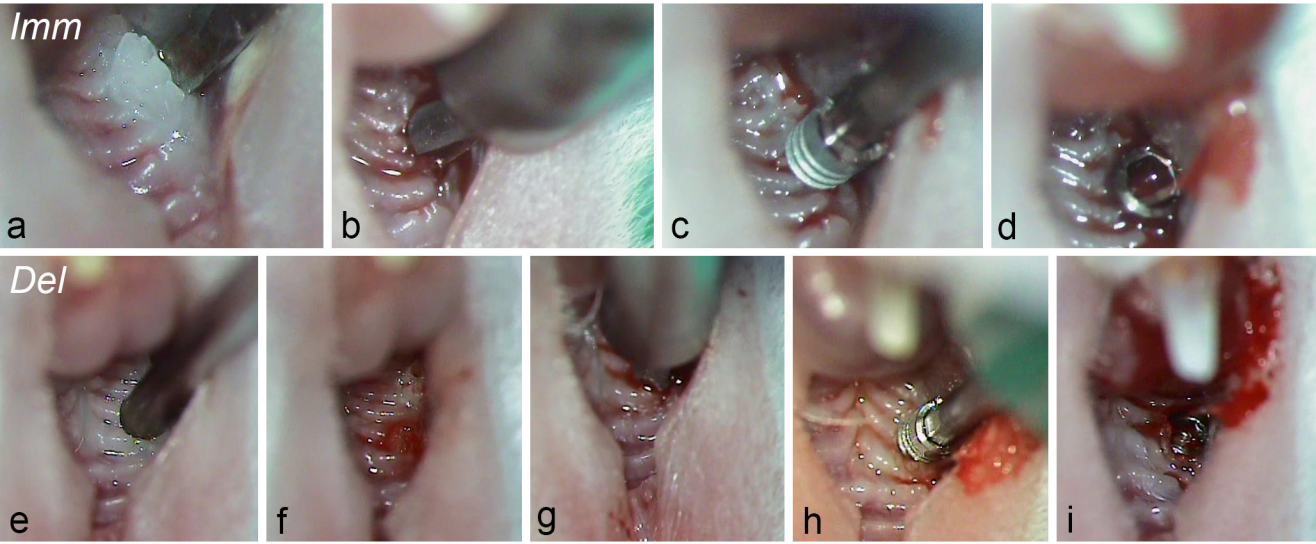

Supplementary Figure 1

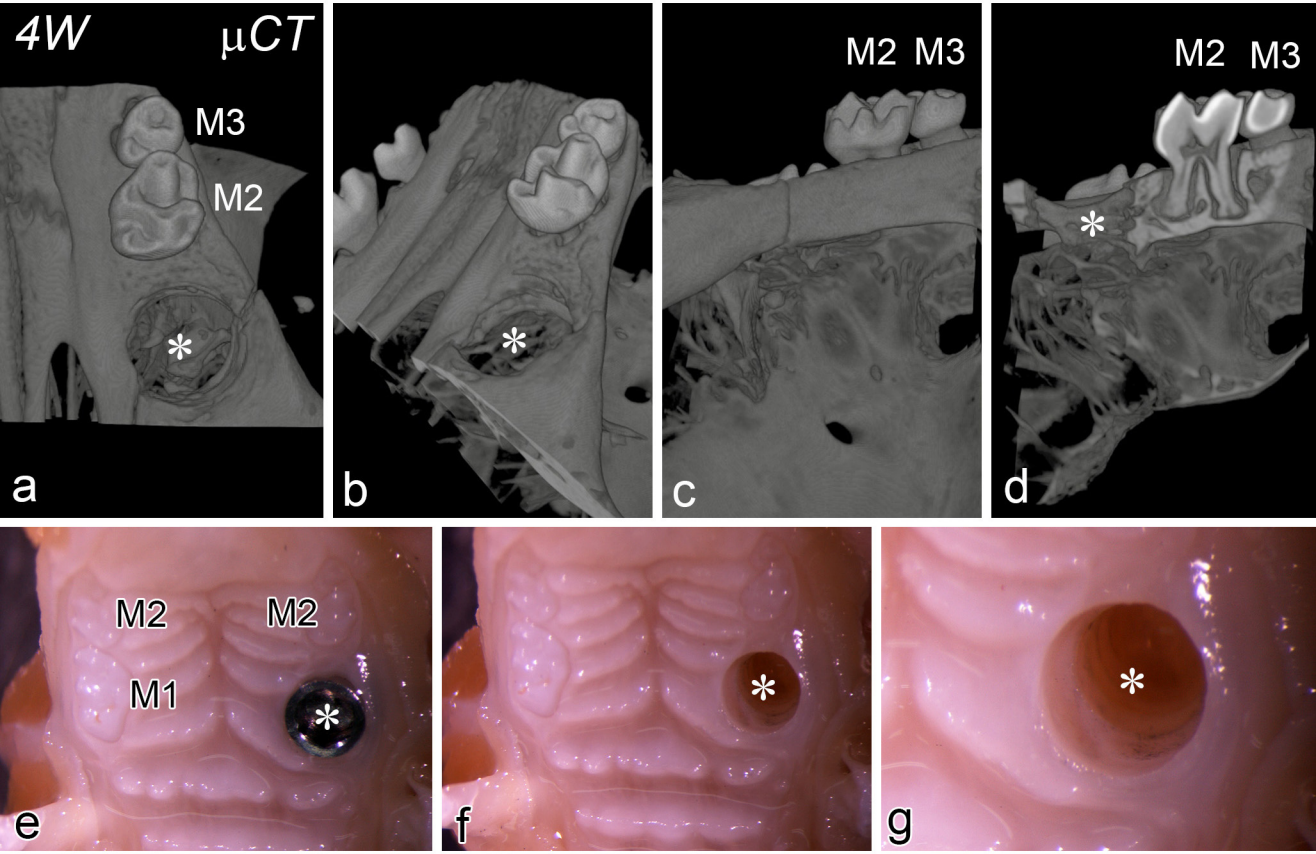

Supplementary Figure 2